X-Ray Crystal Structures and Electronic Aspects of Two Mononuclear Iron(III) Complexes of the Class $Fe^{III}LL'$ with the Quadridentate Ligand L = salen or nta and the Bidendate Ligand L′ = Oxalate [salen = bis(salicylidene)ethylenediamine Anion, H_3nta = *N*,*N*-bis(Carboxymethylglycine)]

Isabelle Malfant,[a] Irène Morgenstern-Badarau,*[a] Michèle Philoche-Levisalles,[b] and Francesc Lloret[c]

[a] *Laboratoire de Chimie Bioorganique et Bioinorganique, URA 1384, Université de Paris-Sud, 91405 Orsay, France*
[b] *Laboratorie de Chimie des Métaux de Transition, URA 419, Université de Paris VI, 75252 Paris Cedex 05, France*
[c] *Departament de Quimica Inorganica, Universitat de Valencia, 46100 Burjassot (Valencia), Spain*

The *X*-ray crystal structures of two mixed-ligand six-co-ordinate iron(III) complexes, $[Fe^{III}(salen)(ox)]pipH$ (**1**) and $[Fe^{III}(nta)(ox)](dabcoH)_2$ (**2**) (ox = oxalate, pipH = piperidinium cation, dabcoH = 1,4-diazabicyclo[2.2.2]octane cation) are characterized by a distorted octahedral co-ordination; the resulting ligand field rhombicity and spin–orbit coupling provide significant quantum mixing of the $S = 5/2$ ground state as revealed by magnetic properties studies.

The chemistry of iron(III) complexes has been extensively investigated and still is of intense interest. One of the main reasons of such a continuous effort in the field is the relevance to iron proteins. Within the class of mixed-ligand six-co-ordinate complexes $Fe^{III}LL'$, with L = a quadridentate ligand and L′ = a bidentate ligand, several molecules have been described with L = the salen Schiff base or a modified salen ligand.[1] With L = nta, one complex has been crystallographically characterized.[2] With the ligand L′ = catecholate, the corresponding salen or nta complexes have been proposed as models for catechol dioxygenase.[2,3] To date no complex of this class has been reported with the oxalate dianion as the bidentate ligand.

In this communication we report the structural, magnetic and EPR characterization of two six-co-ordinate mononuclear iron(III) complexes [Fe^{III}(salen)(ox)]pipH (**1**)[4] and [Fe^{III}(nta)(ox)](dabcoH)$_2$ (**2**), which could be relevant to the understanding of the electronic structure of iron(III)-containing molecules with a distorted octahedral ligand field. Besides of this fundamental interest, the reported study is of potential importance because it can account for structural and electronic factors which influence the reactivity of non-haem centres.

Complex (**1**) was prepared from the reaction between Fe(salen)Cl,[5] oxalic acid and piperidine (1 : 1 : 2 molar ratio) in methanol under reflux for 3 h. The resulting intensely coloured solution was concentrated and allowed to evaporate slowly in air for 3 days to yield well formed reddish-brown crystals. Complex (**2**) was synthesized by the reaction between Fe(nta)·H$_2$O,[6] oxalic acid, and dabco (1 : 1 : 2 molar ratio) in dimethylformamide. The suspension obtained was heated for 4 h in an argon atmosphere, at 90 °C. The resulting yellow solution was allowed to cool slowly to 70 °C and kept at this temperature to yield, after 2 weeks, yellow crystals suitable for *X*-ray analysis.

The structures of (**1**) and (**2**) revealed by *X*-ray crystallography† (Figures 1 and 2) are similar. They consist of discrete octahedra of the anionic species [Fe(salen)ox]$^-$ for (**1**) and [Fe(nta)ox]$^{2-}$ for (**2**) together with pipH$^+$ and two dabcoH$^+$ as counter-ions respectively, which are stabilized by ionic and hydrogen-bond interactions. In both molecules, the oxalate group occupies two *cis*-positions of the octahedron around the metal ion, the six-co-ordination being completed either by the linear bi-anionic salen ligand or by the tripodal tri-anionic nta ligand. The angles around the iron differ from 90° or 180° for an ideal octahedral geometry, owing to the constraints imposed by essentially the accommodation of the oxalate [O(1)–Fe–O(2) = 77.4° for (**1**) and 82.2° for (**2**)]. The distortion of the octahedron is also reflected in the metal–ligand bond lengths. The most striking feature appears in the ligation of the oxalate ligand: (i) an identical and significant difference in the two Fe–O(ox) bond lengths which is *ca.* 0.08 Å in both complexes, with the shorter bond Fe–O(2) being *trans* to the amine ligand Fe–N(1), the longest bond of the octahedron; (ii) a significant difference in the metal–oxalate interaction which appears weaker in complex (**1**) than in complex (**2**) [average values for M–O(ox) bonds are 2.06 Å for (**1**) and 1.98 Å for (**2**)]. These structures are similar to those reported for catecholate complexes.[2,3]

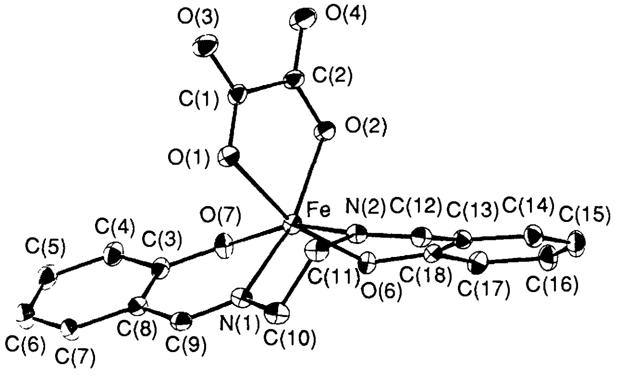

Figure 1. ORTEP projection of the anionic complex [Fe(salen)(ox)]$^-$ at the 50% probability level. Selected bond distances (Å) and angles (°): Fe–O(1) 2.105(4), Fe–O(2) 2.024(4), Fe–N(2) 2.103(4), Fe–O(6) 1.916(3), Fe–O(7) 1.912(5), and Fe–N(1) 2.157(5); O(2)–Fe–O(1) 77.4(1), O(6)–Fe–O(1) 163.3(2), O(7)–Fe–N(2) 159.9(2), N(1)–Fe–O(2) 158.1(2), N(2)–Fe–N(1) 75.3(2), N(1)–Fe–O(6) 112.9(2), and N(1)–Fe–O(7) 85.9(2).

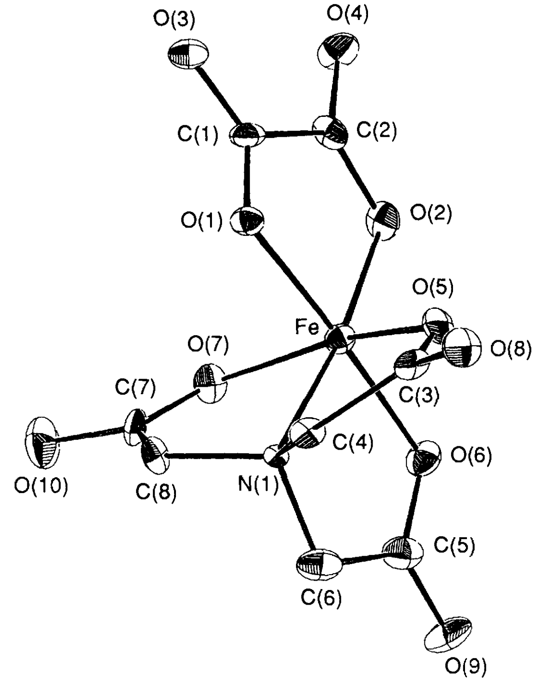

Figure 2. ORTEP projection of the anionic complex [Fe(nta)(ox)]$^{2-}$ at the 50% probability level. Selected bond distances (Å) and angles (°): Fe–O(1) 2.019(9), Fe–O(2) 1.94(1), Fe–O(5) 1.96(1), Fe–O(6) 1.979(9), Fe–O(7) 1.98(1), and Fe–N(1) 2.13(1); O(2)–Fe–O(1) 82.2(4), O(6)–Fe–O(1) 176.4(4), O(7)–Fe–O(5) 158.2(4), N(1)–Fe–O(2) 173.1(4), N(1)–Fe–O(5) 79.8(4), N(2)–Fe–O(6) 85.4(2), and N(1)–Fe–O(7) 78.9(4).

Variable-temperature solid-state magnetic susceptibility studies were performed on powdered samples in the range 4.2—300 K. The effective magnetic moment μ_{eff} [$\mu_{\text{eff}}(T)$ =

---

† *Crystal data* for (**1**): [Fe(salen)(ox)]pipH, $C_{23}H_{26}FeN_3O_6$, M = 496, monoclinic, space group $P2_1/n$, Z = 4, a = 14.302(2), b = 6.960(2), c = 24.387(3) Å, β = 99.07(1)°, U = 2352(1) Å^3. For (**2**): [Fe(nta)(ox)](dabcoH)$_2$, $C_{20}H_{32}FeN_3O_{10}$, M = 558, monoclinic, space group $C2/c$, Z = 8, a = 21.911(4), b = 11.432(4), c = 22.475(7) Å, β = 106.70(2)°, U = 5392(4) Å^3. For both structures, intensity data were measured at 18 °C, with Mo-$K\alpha$ radiation (graphite crystal monochromator) using an Enraf-Nonius CAD-4F diffractometer, with the $\omega/2\theta$ scan method. The structures were solved using the Patterson method and subsequent Fourier maps (SHELX-86) and refined using a blocked least-squares procedure. All atoms except hydrogen were anisotropically refined. Hydrogen atoms were introduced with isotropic overall thermal parameters. The crystals of complex (**2**) appeared to be very sensitive to moisture. The structure determination was carried out on a crystal taken from the solution and sealed in a capillary tube. During the data collection, the intensities of two standard reflections decreased by 35%, and a correction was applied. Because of this sensitivity fewer reflections were used and the results are less accurate for complex (**2**) than for complex (**1**). The structures were refined to R (R_W) values of 0.038 (0.041) for 1955 reflections used with $I > 3\sigma(I)$ for (**1**), and R (R_W) values of 0.083 (0.096) for 1230 reflections used with $I > 3\sigma(I)$ for (**2**). Atomic co-ordinates, bond lengths and angles, and thermal parameters have been deposited at the Cambridge Crystallographic Data Centre. See Notice to Authors, Issue No. 1.

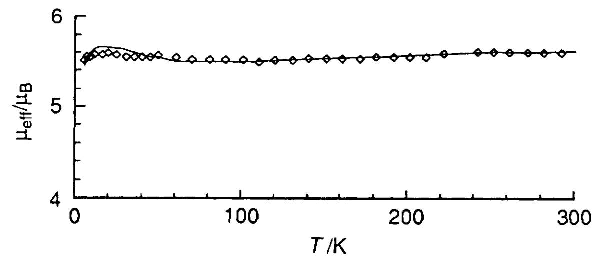

Figure 3. Effective magnetic moment data for complex (**2**) over the temperature range 4.2—300 K. The solid line is the fit of the data to the theoretical susceptibility equations derived from the model described in the text.

$2.828\ (\chi_m T)^{\frac{1}{2}}$, in which χ_m is the corrected molar susceptibility at temperature T] is 5.75 μ_B for (**1**) and 5.65 μ_B for (**2**) at 300 K, remains almost constant over a large temperature range, then decreases to reach 5.65 μ_B for (**1**) and 5.52 μ_B for (**2**), at the lowest temperature (the experimental errors have been estimated to be 0.02 μ_B at high temperature). The striking feature is the deviation of the effective magnetic moment from the typical value of 5.92 μ_B for a pure high-spin $S = 5/2$ ground state, associated with an apparent Curie law behaviour. By considering the high temperature range, where the temperature independence of the effective magnetic moment allows any fine structure or exchange effects to be neglected, the appropriate spin Hamiltonian for pure high-spin iron(III) systems would provide g values smaller than 2. Therefore, the spin Hamiltonian formalism is not an adequate description for the analysis of the reported magnetic properties, especially in the case of complex (**2**) which exhibits the more pronounced effective moment depression (Figure 3). Similar magnetic behaviour has often been reported in the literature and the need for more refined models to explain this effect has been emphasised, in mononuclear systems[7] and also in clusters.[8]

We have developed an alternative model which includes significant orbital contributions to the ground state *via* spin–orbit coupling, following theoretical calculations applied to iron(III) configurations,[9] proposed for the study of hemoproteins,[10] and of porphyrin systems.[11] The quantum mixing we have considered implies perturbations of the sextet ground state $S = 5/2$ by two nearly degenerate, rhombically split quartet components, themselves perturbed by a nearby doublet level. The fit of the data for complex (**2**) to the derived theoretical susceptibility equations, which also account for average field orientation,[12] provides estimates for the quantum mixing of the ground state Kramers doublet: 87% ($S = 5/2$), 12% ($S = 3/2$), 1% ($S = 1/2$).

For greater reliability, magnetization measurements were performed at 5 K in the range 0.5—4 T, on compound (**2**). An apparent saturation is displayed for $H > 1.5$ T to reach $M/N\mu_B = 3$. The data have been accurately reproduced with the set of parameters deduced from susceptibility calculations.

X-Band EPR spectra were run at 4.2 K on powdered samples. Both complexes exhibit broad features. The spectrum of complex (**2**) which is better resolved displays a bump at $g \sim 9$, an intense resonance at $g \sim 4.3$, and a weaker one at $g \sim 1$. Our calculations give the effective g values of 9.4 for the lower Kramers doublet, 3.9, 4.9, 4.3 for the middle doublet, and 9.9, 0.9 for the upper one, in agreement with the main EPR features. The other calculated transitions occur at g values smaller than 0.75, corresponding to magnetic fields which were not available.

The detailed analysis of the electronic properties of such iron(III) complexes characterized by a rhombically distorted octahedral ligand field permits estimates of the intermediate spin configuration (and of the low spin one to a lesser extent) involved in the high-spin ground state. Such quantum mixing is more pronounced in the case of a stronger ligand field interaction as revealed by the structural features. Tunnelling of such interactions is required to emphasize the magnitude of the orbital contribution to the ground state. Recently, an exhaustive analysis of magnetic circular dichroism data also in terms of ligand field and spin–orbit coupling has been developed to account for the electronic structure of the superoxide dismutase iron(II) site.[13]

Received, 14th May 1990; Com. 0/02139C

References

1 M. Nakamura, T. Itoh, H. Okawa, and S. Kida, *J. Inorg. Nucl. Chem.*, 1981, **43**, 2281; R. H. Heistand, R. B. Lauffer, E. Fikrig, and L. Que, *J. Am. Chem. Soc.*, 1982, **104**, 2789; R. B. Lauffer, R. H. Heistand, and L. Que, *Inorg. Chem.*, 1983, **22**, 50.

2 L. S. White, P. V. Nilson, L. H. Pignolet, and L. Que, *J. Am. Chem. Soc.*, 1984, **106**, 8312.

3 L. Que, R. C. Kolanczyck, and L. S. White, *J. Am. Chem. Soc.*, 1987, **109**, 5373; D. D. Cox and L. Que, *J. Am. Chem. Soc.*, 1988, **110**, 8085.

4 A structure obtained by isomorphous replacement for the coordinates of the isostructural chromium complex has been proposed by two of us: F. Lloret, M. Julve, M. Mollar, I. Castro, J. Lattore, J. Faus, X. Solans, and I. Morgenstern-Badarau, *J. Chem. Soc., Dalton Trans.*, 1989, 729.

5 M. Gerloch and F. F. Mabbs, *J. Chem. Soc. A*, 1967, 1900.

6 M. Krishnamurthy and K. B. Morris, *J. Inorg. Nucl. Chem.*, 1972, **34**, 719.

7 See for example: K. J. Berry, P. E. Clark, K. S. Murray, C. J. Raston, and A. H. White, *Inorg. Chem.*, 1983, **22**, 3928; C. J. Carrano, K. Spartalian, G. V. N. Appa Rao, V. L. Pecoraro, and M. Sundaralingam, *J. Am. Chem. Soc.*, 1985, **107**, 1651; J. N. Burstyn, J. A. Roe, A. R. Miksztal, B. A. Shaevitz, G. Lang, and J. S. Valentine, *J. Am. Chem. Soc.*, 1988, **110**, 1382.

8 B. S. Snyder, G. S. Patterson, A. J. Abrahamson, and R. H. Holm, *J. Am. Chem. Soc.*, 1989, **111**, 5214.

9 J. S. Griffith, in 'The Theory of Transition Metal Ions,' Cambridge University Press; Cambridge, 1964; J. S. Griffith, *Mol. Phys.*, 1964, **8**, 213; G. Harris, *Theor. Chim. Acta*, 1968, **10**, 119; G. Harris, *Theor. Chim. Acta*, 1968, **10**, 155.

10 M. Weissbluth, *Struct. Bonding (Berlin)*, **2**, pp. 1–125; M. M. Maltempo and T. H. Moss, *Q. Rev. Biophys.*, 1976, **9**, 181; C. E. Schulz, R. Rutter, J. T. Sage, P. G. Debrunner, and L. P. Hager, *Biochemistry*, 1984, **23**, 4743.

11 C. A. Reed, T. Mashiko, S. P. Bently, M. E. Kastner, W. R. Scheidt, K. Spartalias, and G. J. Lang, *J. Am. Chem. Soc.*, 1979, **101**, 2948; W. R. Scheidt, D. K. Geiger, R. G. Hayes, and G. Lang, *J. Am. Chem. Soc.*, 1983, **105**, 2625; W. R. Scheidt, S. R. Osvath, Y. J. Lee, C. A. Reed, B. Shaevitz, and G. V. Gupta, *Inorg. Chem.*, 1989, **28**, 1591; S. Mitra, V. R. Marathe, and R. Birdy, *Chem. Phys. Lett.*, 1983, **96**, 103; P. Bertrand, F. X. Theodule, J. P. Gayda, J. Mispelter, and M. Momenteau, *ibid.*, 1983, **102**, 442; G. E. Toney, A. Gold, J. Savin, W. ter Haar, R. Sangaiah, and W. E. Hatfield, *Inorg. Chem.*, 1984, **23**, 4350.

12 V. R. Marathe and S. Mitra, *Chem. Phys. Lett.*, 1984, **27**, 103; A. K. Gregson, *Aust. J. Chem.*, 1980, **33**, 2547.

13 J. W. Whittaker and E. I. Solomon, *J. Am. Chem. Soc.*, 1988, **110**, 5329.